ground water

Potential Contaminant Pathways from

1290 kg/m^3, or more than 29% higher than freshwater. The upward force would equal the difference in weight between the injected ßuid and displaced brine. As an example, if 10,000,000 L does not return to the surface as ßowback (Jehn 2011), the difference in mass between the volume of fracking ßuid and displaced brine is approximately 3,000,000 kg, which would cause an initial upward force. The density difference would dissipate as the salt concentration in the fracking ßuid increases due to diffusion across the boundary between the ßuid and the brine.

In just Pennsylvania, more than 180,000 wells had been drilled prior to any requirement for documenting their location (Davies 2011), therefore the location of many wells is unknown and some have probably been improperly abandoned. These pathways connect aquifers through otherwise continuous aquitards; overpressurization of lower aquifers due to injection near the well pathway could cause rapid transport to higher aquifers (Lacombe et al. 1995). In the short fracking period, the region that is overpressurized remains relatively close to the gas well (see modeling analysis below), therefore it should be possible for the driller to locate nearby abandoned wells that could be affected by fracking. This article shale (Fisher and Warpinski 2011). These fractures could contact higher conductivity sandstone, natural fractures, or unplugged abandoned wells above the target shale. Also, ßuids could reach surrounding formations just because of the volume injected into the shale, which must displace natural ßuid, such as the existing brine in the shale.

Analysis of Potential Transport along Pathways

Fracking could cause contaminants to reach overlying formations either by fracking out of formation, connecting fractures in the shale to overlying bedrock, or by simple displacement of ßuids from the shale into the overburden. Advective transport, considered as simple particle velocity, will manifest if there is a signiÞcant vertical component to the regional hydraulic gradient.

Numerical modeling, completed with the MODF LOW-2000 code (Harbaugh et al. 2000), provides ßexibility to consider potential conceptual ßow scenarios, but should be considered interpretative (Hill and Tiedeman 2007). The simulation considers the rate of vertical transport of contaminants to near the surface for the different conceptual models, based on an expected, simpliÞed, real-

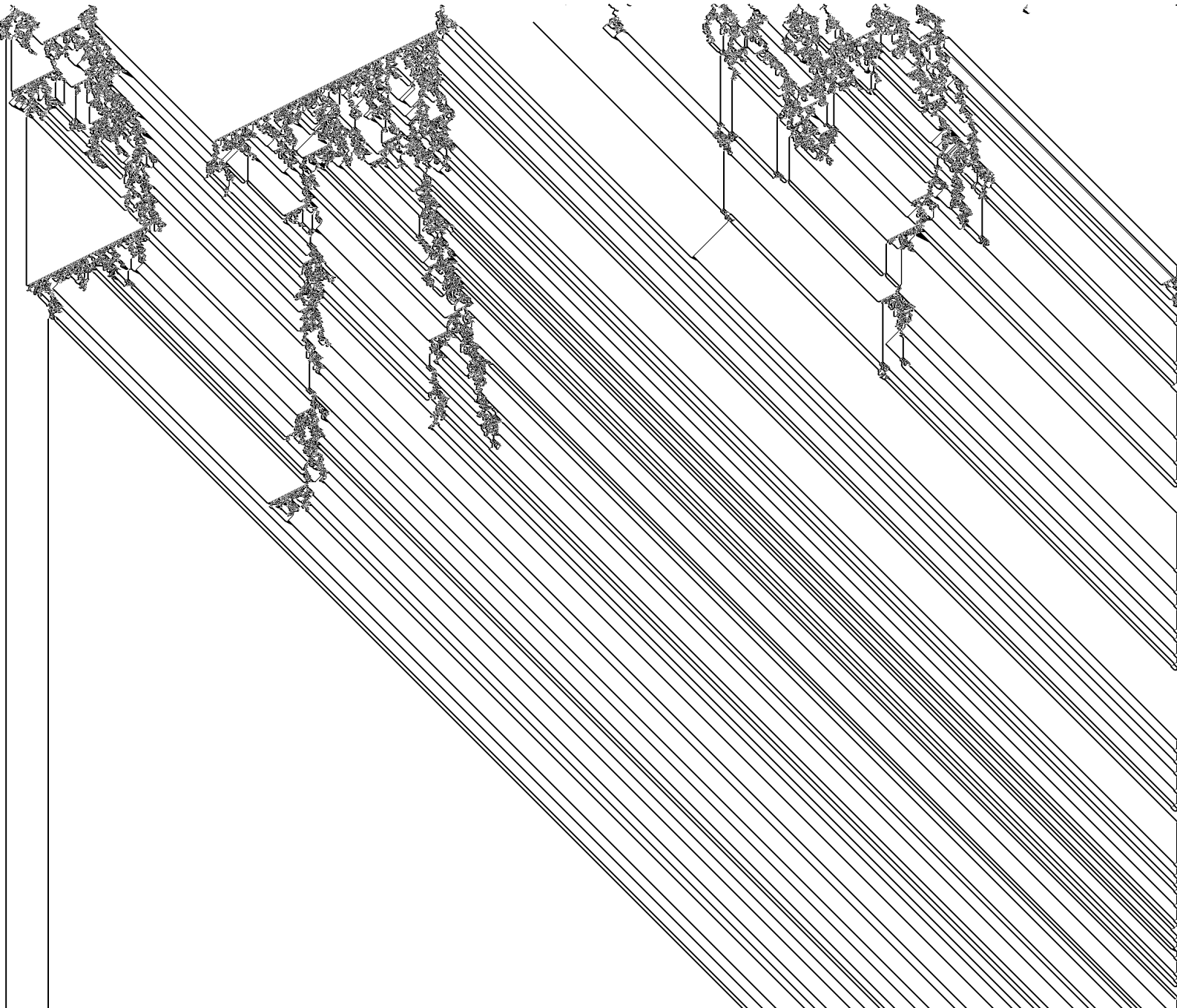

to be 6-m thick. The fault is an attempt at considering fracture ßow, but the simulation treats the 6-m wide fault zone as homogeneous, which could underestimate the real transport rate in fracture-controlled systems which could be highly affected by dispersion. The simulation also ignores diffusion between the fracture and the adjacent shale matrix (Konikow 2011).

There are Þve conceptual models of ßow and transport of natural and post-fracking transport from the level of the Marcellus shale to the near-surface to consider herein:

1. The natural upward advective ßow due to a head drop of 30 m from below the Marcellus shale to the ground surface, considering the variability in both shale and overburden K. This is a steady state solution for upward advection through a 30-m thick shale zone and 1500-m overburden. Table 1 shows the chosen K values for shale and sandstone.
2. Same as number 1, but with a vertical fracture connecting the shale with the surface, created using a high-conductivity zone in a row of cells extending through all from above the shale to the surface. This emulates the conceptual model postulated for ßow into the alluvial aquifers near stream channels, the location of which may be controlled by faults (Williams et al. 1998). The fault K varies from 10 to 1000 times the surrounding bulk sandstone K (K_{ss}).
3. This scenario tests the effect of extensive fracturing in the Marcellus shale by increasing the shale K (K_{sh}) from 10 to 1000 times its native value over an extensive area. This transient solution starts with initial conditions being a steady state solution from scenario 1. The K_{sh} increases from 10 to 1000 times at the beginning of the simulation, to represent the relatively instantaneous change on the regional shale hydrogeology imposed by the fracking. The simulation estimates both the changes in ßux and the time for the system to reach equilibrium.
4. As number 3, considering the effect of the same changes in shale properties but with a fault as in number 2.
5. This scenario simulates the actual injection of 13 to 17 million liters of ßuid in 5 d into fractured shale from a horizontal well with and without a fault.

Table 1
Sandstone (ss) and Shale (sh) Conductivity (K) (m/d) and the Steady State Flux (m^3/d) for Model 1 Scenarios

Flux	K_{ss}	K_{sh}
1.7	0.1	0.00001
1.8	0.5	0.00001
1.9	1	0.00001
1.9	5	0.00001
2.0	10	0.00001
2.0	50	0.00001
2.0	100	0.00001
1.7	0.1	0.00001
9.5	0.1	0.00005
19.0	0.1	0.0001
81.2	0.1	0.0005
135.9	0.1	0.001
291.5	0.1	0.005
340.9	0.1	0.01
394.3	0.1	0.05
401.8	0.1	0.1
409.2	0.1	0.5
40.7	0.001	0.1
186.0	0.005	0.1
339.1	0.01	0.1
988.3	0.05	0.1
1297.3	0.1	0.1
1748.0	0.5	0.1
1826.1	1	0.1
1902.8	5	0.1
1915.4	10	0.1
338.3	0.1	0.01
984.1	0.5	0.01
1292.5	1	0.01
1731.5	5	0.01
1816.0	10	0.01
17.4	1	0.0001
86.3	1	0.0005
176.7	1	0.001
775.1	1	0.005
1292.5	1	0.01
2746.8	1	0.05
3183.2	1	0.1
3650.5	1	0.5
3719.9	1	1

Model Setup

The model domain was 150 rows and columns spaced at 3 m to form a 450-m square (Figure 2) with 50 layers bounded with no ßow boundaries. The 30-m thick shale was divided into 10 equal thickness layers from layer 40 to 49. The overburden layer thickness varied from 3 m just above the shale to layer 34, 6 m from layer 33 to 29, 9 m from layer 28 to 26, 18 m in layer 25, 30 m from layer 24 to 17, 60 m from layer 16 to 6, 90 m from layer 5 to 3, and 100 m in layers 2 and 1. A 6-m wide column from layer 39 to the surface is added for some scenarios in the center two rows to simulate a higher K fault.

The model simulated vertical ßow between constant head boundaries in layers 50 and 1, as a source and sink, so that the overburden and shale properties control the ßow. The head in layers 50 and 1 was 1580 and 1550 m, respectively, to create a gradient of 0.019 over the proÞle. Varying the gradient would have much less effect on transport than changing K over several orders of magnitude and was therefore not done.

Scenario 5 simulates injection using a WELL boundary in layer 44, essentially the middle of the shale, from columns 25 to 125 (Figure 2). It injects 15 million liters over one 5-d stress period, or 3030 m^3/d into 101 model cells at the WELL. The modeled K_{sh} was changed to its

EPAPAV0058600

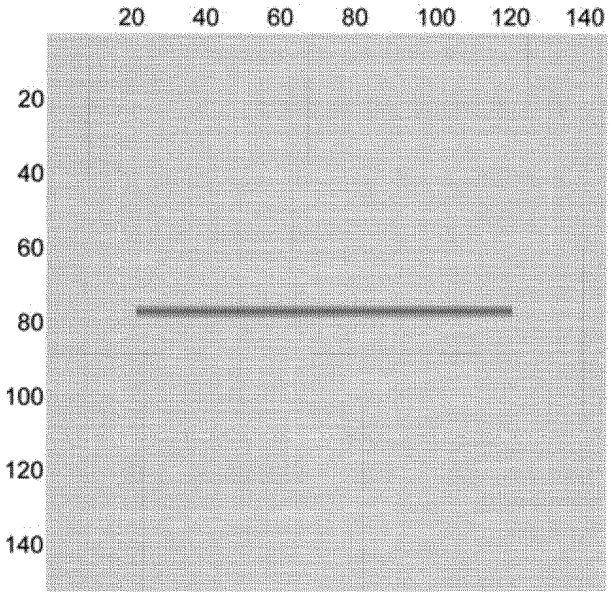

Figure 2. Model grid through layer 44 showing the horizontal injection WELL (red) and DRAIN cells (yellow) used to simulate flowback. There is only one monitoring well because the off-center well is not used in layer 44.

assumed fracked value at the beginning of the simulation. Simulating high rate injection generates very high heads in the model domain, similar to that found simulating oil discharging from the well in the Deepwater Horizon crisis (Hsieh 2011) and water quality changes caused by underground coal gasiþcation (Contractor and El-Didy 1989). DRAIN boundaries on both sides of the WELL simulated return ßow for 60 d after the completion of (Figure 2), after which the DRAIN was deactivated. The 60 d were broken into four stress periods, 1, 3, 6, and 50 d long, to simulate the changing heads and ßow rates. DRAIN conductance was calibrated so that 20% of the injected volume returned within 60 d to emulate standard industry practice (Alleman 2011; NYDEC 2009). Recovery, continuing relaxation of the head at the well and the adjustment of the head distribution around the domain, occurred during the sixth period which lasted for 36,500 d.

There is no literature guidance to a preferred value for fractured shale storage coefþcient, so I estimated S with a sensitivity analysis using scenario 3. With fractured K_{sh} equal to 0.001 m/d, two orders of magnitude higher than the in situ value, the time to equilibrium resulting from simulation tests of three fractured shale storage coefþcients, 10^{-3}, 10^{-5}, and 10^{-7}/m, varied twofold (Figure 3). The slowest time to equilibrium was for $S = 10^{-3}$/m (Figure 3), which was chosen for the transient simulations because more water would be stored in the shale and ßow above the shale would change the least.

Results

Scenario 1

Table 1 shows the conductivity and ßux values for various scenarios. The steady state travel time

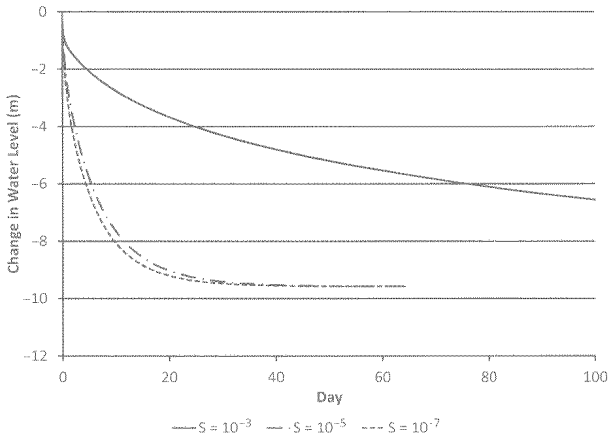

Figure 3. Sensitivity of the modeled head response to the storage coefficient used in the fractured shale for model layer 39 just above the shale.

for a particle through 1500 m of sandstone and shale equilibrates with one of the formations controlling the advection (Figure 4). For example, when the K_{sh} equals 1×10^{-5} m/d, transport time does not vary with K_{ss}. For K_{ss} at 0.1 m/d, transport time for varying K_{sh} ranges from 40,000 to 160 years. The lower travel time estimate is for K_{sh} similar to that found by Schulze-Makuch et al. (1999). The shortest simulated transport time of about 20 years results from both the sandstone and shale K equaling 1 m/d. Other sensitivity scenarios emphasize the control exhibited by one of the media (Figure 4). If K_{sh} is low, travel time is very long and not sensitive to K_{ss}.

Scenario 2

The addition of a fault with K one to two orders of magnitude more conductive than the surrounding sandstone increased the particle travel rate by about 10 times (compare Figure 5 with Figure 4). The fault K controlled the transport rate for K_{sh} less than 0.01 m/d. A highly

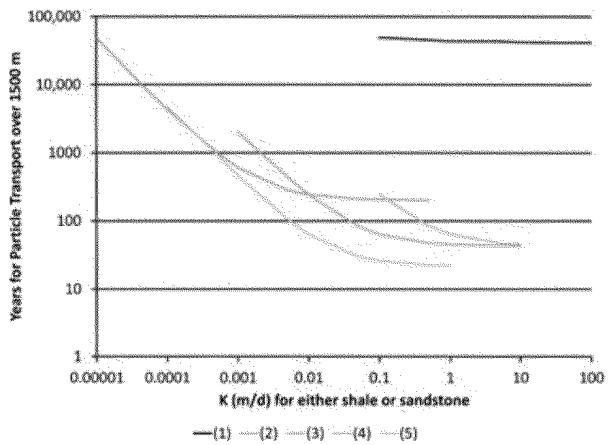

Figure 4. Sensitivity of particle transport time over 1500 m for varying shale and sandstone vertical K. Effective porosity equals 0.1. (1)—varying K_{ss}, $K_{sh} = 10^{-5}$ m/d; (2)—varying K_{ss}, $K_{sh} = 0.1$ m/d; (3)—varying K_{ss}, $K_{sh} = 0.1$ m/d; (4)—varying K_{ss}, $K_{sh} = 0.01$ m/d; and (5)—varying K_{ss}, $K_{sh} = 1.0$ m/d.

EPAPAV0058601

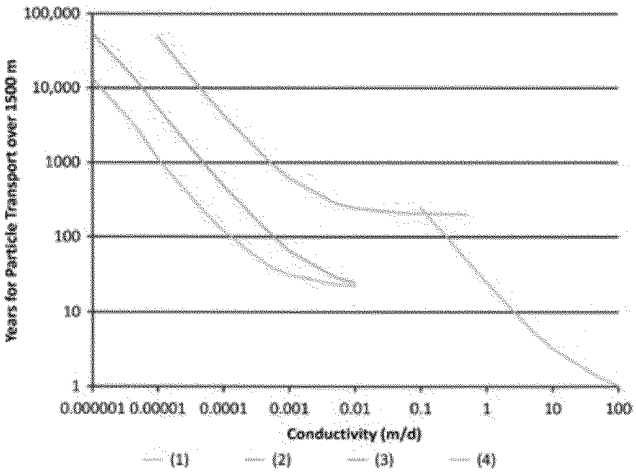

Figure 5. Variability of transport through various scenarios of changing the K for the fault or shale. Effective porosity equals 0.1. (1)—varying K_{sh}, K_{sh} = 0.01 m/d; (2)—varying K_{sh}, K_{sh} = 0.1 m/d; (3)—no fault; (4)—varying K fault, K_{sh} = 0.1 m/d, K_{sh} = 0.01 m/d. Unless specified, the vertical fault has K = 1 m/d for variable K_{sh}.

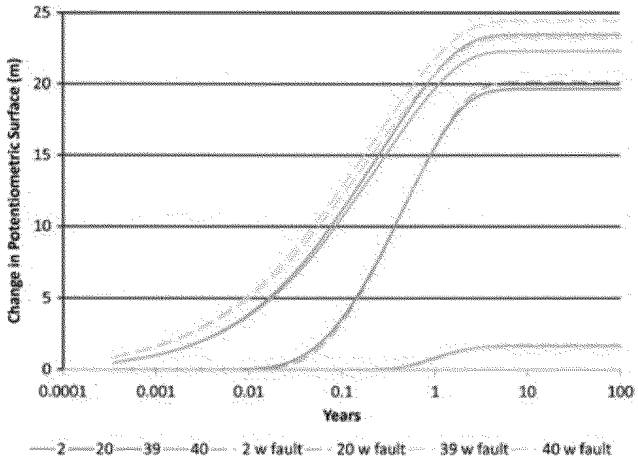

Figure 6. Monitoring well water levels for specified model layers due to fracking of the shale; monitor well in the center of the domain, including in the fault, K of the shale changes from 0.00001 to 0.01 m/d at the beginning of the simulation.

conductive fault could transport ßuids to the surface in as little as a year for K_{sh} equal to 0.01 m/d (Figure 5). However, a fault did not signiÞcantly change the overall model ßux, so with fault values are not shown in Table 1.

Scenarios 3 and 4

Scenarios 3 and 4 estimate the time to establish a new equilibrium once the K_{sh} changes, due to fracking, between values speciÞed in scenarios 1 and 2. Equilibrium times vary by model layer as the changes propagate through the domain, and ßux rate for the simulated changes imposed on natural background conditions. The fracking-induced changes cause a signiÞcant decrease in the head drop across the shale and the time for adjustment of the potentiometric surface to a new steady state depends on the new shale properties.

The time to equilibrium for one scenario 3 simulation, K_{sh} changing from 10^{-5} to 10^{-2} m/d with K_{ss} equal to 0.1 m/d, varied from 5.5 to 6.5 years, depending on model layer (Figure 6). Near the shale (layers 39 and 40), the potentiometric surface increased from 23 to 25 m reßecting the decreased head drop across the shale. One hundred meters higher, in layer 20, the potentiometric surface increased about 20 m. Simulation of scenario 4, with a fault with K = 1 m/d, decreased the time to equilibrium to from 3 to 6 years within the fault zone, depending on model layer (Figure 6). Highly fractured sandstone would allow more vertical transport, but advective ßow would also increase so that the base K_{ss} would control the overall rate.

The ßux across the upper boundary changed within 100 years for scenario 3 from 1.7 to 345 m^3/d, or 0.000008 to 0.0017 m/d, reßecting control by K_{ss}. There is little difference in the equilibrium ßuxes between scenario 3 and 4 indicating that the fault primarily affects the time to equilibrium rather than the long-term ßow rate.

Scenario 5: Simulation of Injection

The injection scenarios simulate 15 million liters entering the domain at the horizontal well and the subsequent potentiometric surface and ßux changes throughout. The highest potentiometric surface increases (highest injection pressure) occurred at the end of injection (Figure 7), with a 2400 m increase at the horizontal well. The simulated peak pressure both decreased and occurred longer after the cessation of injection with distance from the well (Figures 7 and 8). The pressure at the well returned to within 4 m of pre-injection levels in about 300 d (Figure 7). After injection ceases, the peak pressure simulated further from the well occurs longer from the time of cessation, which indicates there is a pressure divide beyond which ßuid continues to ßow away from the well bore while within which the ßuid ßows toward the well bore. The simulated head returned to near pre-injection levels slower with distance from the well (Figure 7), with levels at the edge of the shale (layer 40) and in the near-shale sandstone (layer 39) requiring several hundred days to recover. After recovering from injection, the potentiometric surface above the shale increased in response to ßux through the shale adjusting to the change in shale properties (Figure 8), as simulated in scenario 3. The scenario required about 6000 d (16 years) for the potentiometric surface to stabilize at new, higher, levels (Figure 8). Removing the fault from the simulation had little effect on the time to stabilization, and is not shown.

Prior to injection, the steady ßux for in situ shale (K_{sh} = 10^{-5} m/d) was generally less than 2 m^3/d and varied little with K_{ss} (Figure 4). Once the shale was fractured, the sandstone controlled the ßux which ranges from 38 to 135 m^3/d as K_{ss} ranges from 0.01 to 0.1 m/d (Figure 9), resulting in particle travel times of 2390 and 616 years, respectively. More conductive shale would allow faster transport (Figure 4). Adding a fault to the scenario with K_{ss} equal to 0.01 m/d increased the ßux to approximately 63 m^3/d and decreased the particle travel

EPAPAV0058602

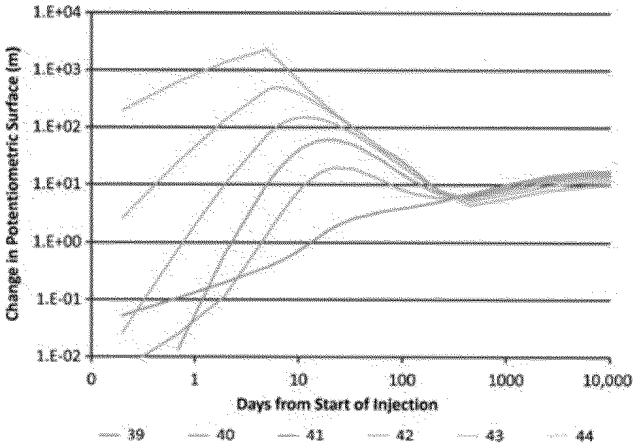

Figure 7. Simulated potentiometric surface changes by layer for specified injection and media properties. The monitoring point is in the center of the domain. Fault is included. K_{sh} = 0.01 m/d, K_{sh} = 0.001 m/d. S (fractured shale) = 0.001/m, S (ss) = 0.0001/m.

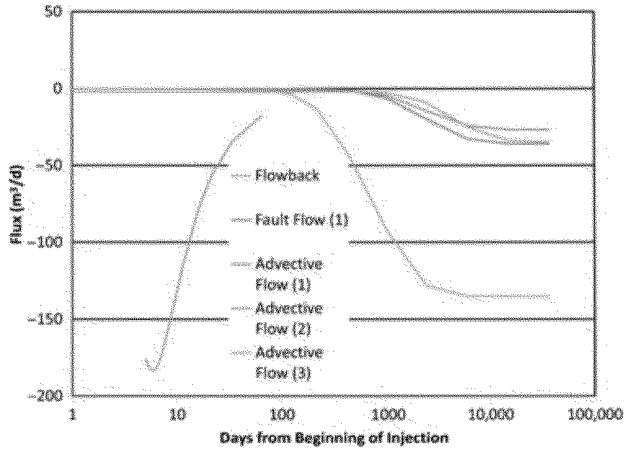

Figure 9. Comparison of flux for three scenarios. Flowback is the same for all scenarios. (1): Kss = 0.01 m/d, Ksh = 0.001 m/d, Fault K = 1m /d;(2):K ss = 0.01 m/d, Ksh = 0.001 m/d, no fault; (3) Kss = 0.1 m/d, Ksh = 0.001 m/d, no fault.

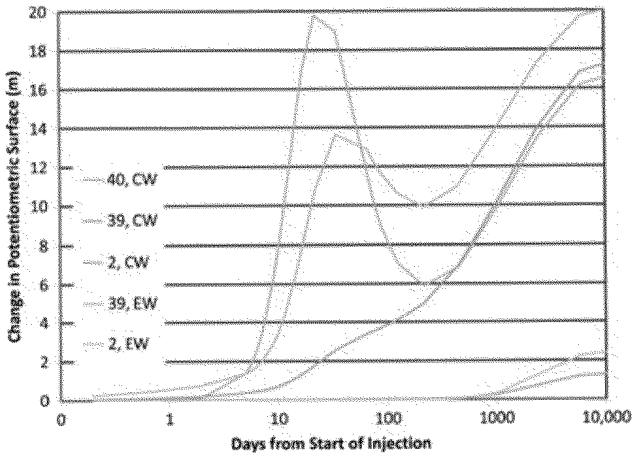

Figure 8. Simulated potentiometric surface changes for layers within the shale and sandstone. CW is center monitoring well and EW is east monitoring well, about 120 m from the centerline. Fault is included. The line for layer 2, CW plots beneath the line for layer 2, EW. K_{ss} = 0.01 m/d, K_{sh} = 0.001 m/d, S (fractured shale) = 0.001/m, S (ss) = 0.0001/m.

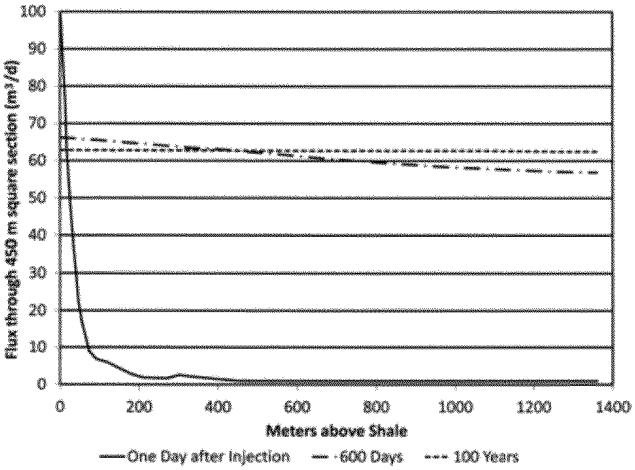

Figure 10. Upward flux across the domain section as a function of distance above the top of the shale layer. Cross section is 202,500 m^2.

time to 31 years. Approximately, 36 m^3/d ßowed through the fault (Figure 9). The fault properties control the particle travel time, especially if the fault K is two or more orders of magnitude higher than the sandstone.

Simulated ßowback varied little with K_{sh} because it had been calibrated to be 20% of the injection volume. A lower storage coefÞcient or higher K would allow the injected ßuid to move further from the well, which would lead to less ßowback.

Vertical ßux through the overall section with a fault varies signiÞcantly with time, due to the adjustments in potentiometric surface. One day after injection, vertical ßux exceeds signiÞcantly the pre-injection ßux about 200 m above the shale (Figure 10). After 600 d, the vertical ßux near the shale is about 68 m^3/d and in layer 2 about 58 m^3/d; it approaches steady state through all sections after 100 years with ßux equaling about 62.6 m^3/d. The 100-year ßux is 61.5 m^3/d higher than the pre-injection ßux because of the changed shale properties.

Discussion

The interpretative modeling completed herein has revealed several facts about fracking. First, MODFLOW can be coded to adequately simulate fracking. Simulated pressures are high, but velocities even near the well do not violate the assumptions for Darcian ßow. Second, injection for 5 d causes extremely high pressure within the shale. The pressure decreases with distance from the well. The time to maximum pressure away from the well lags the time of maximum pressure at the well. The pressure drops back to close to its pre-injection level

EPAPAV0058603

at the well within 300 d, indicating the injection affects the ßow for signiÞcantly longer periods than just during the fracking operation. Although the times may vary based on media properties, the difference would be at most a month or so, based on the various combinations of properties simulated. The system transitions within 6 years due to changes in the shale properties. The equilibrium transport rate would transition from a system requiring thousands of years to one requiring less than 100 years within less than 10 years.

Third, most of the injected water in the simulation ßows vertically rather than horizontally through the shale. This reßects the higher K_{ss} 20 m above the well and the no ßow boundary within 225 m laterally from the well, which emulates in situ shale properties that would manifest at some distance in the shale.

Fourth, the interpretative model accurately and realistically simulates long-term steady state ßow conditions, with an upward ßow that would advect whatever conservative constituents exist at depth. Using low, unfractured K values, the transport simulation may correspond with advective transport over geologic time although there are conditions for which it would occur much more quickly (Figure 4). If the K_{sh} is 0.01 m/d, transport could occur on the order of a few hundreds of years. Faults through the overburden could speed the transport time considerably. Reasonable scenarios presented herein suggest the travel time could be decreased further by an order of magnitude.

Fifth, fracking increases the K_{sh} by several orders of magnitude. Out-of-formation fracking (Fisher and Warpinski 2011) would increase the K in the overburden, thereby changing the regional hydrogeology. Vertical ßow could change over broad areas if the expected density of wells in the Marcellus shale region (NYDEC 2009) actually occurs.

Sixth, if newly fractured shale or out-of-formation fractures come close to contacting fault fracture zones, contaminants could reach surface areas in tens of years, or less. Faults can decrease the simulated particle travel time several orders of magnitude.

Conclusion

Fracking can release ßuids and contaminants from the shale either by changing the shale and overburden hydrogeology or simply by the injected ßuid forcing other ßuids out of the shale. The complexities of contaminant transport from hydraulically fractured shale to near-surface aquifers render estimates uncertain, but a range of interpretative simulations suggest that transport times could be decreased from geologic time scales to as few as tens of years. Preferential ßow through natural fractures fracking-induced fractures could further decrease the travel times to as little as just a few years.

There is no data to verify either the pre- or post-fracking properties of the shale. The evidence for potential vertical contaminant ßow is strong, but there are also almost no monitoring systems that would detect contaminant transport as considered herein. Several improvements could be made.

- Prior to hydraulic fracturing operations, the subsurface should be mapped for the presence of faults and measurement of their properties.
- A reasonable setback distance from the fracking to the faults should be established. The setback distance should be based on a reasonable risk analysis of fracking increasing the pressures within the fault.
- The properties of the shale should be veriÞed, post-fracking, to assess how the hydrogeology will change.
- A system of deep and shallow monitoring wells and piezometers should be established in areas expecting signiÞcant development, before that development begins (Williams 2010).

Acknowledgments

This research was funded by the Park Foundation and Catskill Mountainkeepers. The author thanks Anthony Ingraffea, Paul Rubin, Evan Hansen, two anonymous reviews, and the journal editor for helpful comments on this article.

References

Alleman, D. 2011. Water used for hydraulic fracturing: Amounts, sources, reuse, and disposal. In *Hydraulic Fracturing of the Marcellus Shale*, National Groundwater Association short course. Baltimore, Maryland.

Annunziatellis, A., S.E. Beaubien, S. Bigi, G. Ciotoli, M. Coltella, and S. Lombardi. 2008. Gas migration along fault systems and through the vadose zone in the Latera calder (central Italy): Implications for CO_2 geological storage. *International Journal of Greenhouse Gas Control* 2; 353–372. DOI: 10.1016/j.ijggc.2008.02.003.

Arthur, J.D., B. Bohm, and M. Layne. 2008. *Hydraulic Fracturing Consideration for Natural Gas Wells of the Marcellus Shale.* Cincinnati, Ohio: Ground Water Protection Council.

Boyer, C., J. Kieschnick, R. Suarez-Rivera, R.E. Lewis, and G. Waters. 2006. Producing gas from its source. *Oilfields Review* 18, no. 3: 36–49.

Breen, K.J., K. Revesz, F.J. Baldassare, and S.D. McAuley. 2007. Natural gases in ground water near Tioga Junction, Tioga County, north-central Pennsylvania—Occurrence and use of isotopes to determine origins. ScientiÞc Investigations Report Series 2007-5085. Reston, Virginia: U.S. Geological Survey.

Caine, J.S., J.P. Evans, and C.B. Forster. 1996. Fault zone architecture and permeability structure. *Geology* 24, no. 11: 1025–1028.

Contractor, D.N., and S.M.A. El-Didy. 1989. Field application of a Þnite-element water-quality model to a coal seam with UCG burns. *Journal of Hydrology* 109: 57–64.

Davies, R.J. 2011. Methane contamination of drinking water caused by hydraulic fracturing remains unproven. *Proceedings of the National Academy of Sciences USA* 108: E871.

DiGiulio, D.C., R.T. Wilkin, C. Miller, and G. Oberly. 2011. *DRAFT: Investigation of Ground Water Contamination near Pavillion, Wyoming.* Ada, Oklahoma: U.S. Environmental Protection Agency, OfÞce of Research and Development.

Dresel, P.E., and A.W. Rose. 2010. Chemistry and origin of oil and gas well brines in western Pennsylvania. 4th ser., Open-File Report OFOG 10–01.0, 48. Harrisburg: Pennsylvania Geological Survey.

EPAPAV0058604

Edward, K.L., and S. Weisset. 2011. Marcellus shale hydraulic fracturing and optimal well spacing to maximize recovery and control costs. Paper 140463 in *SPE Hydraulic Fracturing Technology Conference*, January 24–26, 2011, The Woodlands, Texas.

Energy Information Administration (EIA). 2009. *Annual Energy Outlook with Projections to 2030.* Washington, D.C.: U.S. Department of Energy. http://www.eia.doe.gov/oiaf/aeo/ (accessed May 23, 2011).

Engelder, T., G.G. Lash, and R.S. Uzcategui. 2009. Joint sets that enhance production from Middle and Upper Devonian gas shales of the Appalachian Basin. *AAPG Bulletin* 93, no. 7: 857–889.

Environmental Protection Agency (EPA). 1987. Report to congress, management of wastes from the exploration, development, and production of crude oil, natural gas, and geothermal energy, volume 1 of 3, oil and gas. Washington, DC: EPA.

Etiope, G., and G. Martinelli. 2002. Migration of carrier and trace gases in the geosphere: an overview. *Physics of the Earth and Planetary Interiors* 129: 3–4.

Fisher, K., and N. Warpinski. 2011. Hydraulic fracture-height growth: real data. Paper SPE 145949 presented at the Annual Technical Conference and Exhibition, Denver, Colorado. DOI: 10.2118/145949-MS.

Gold, D. 1999. Lineaments and their interregional relationships. In *The Geology of Pennsylvania*, ed. C.H. Schultz, 307–313. Harrisburg: Pennsylvania Department of Conservation and Natural Resources.

Halford, K.J., and R.T. Hanson. 2002. User guide for the drawdown-limited, multi-node well (MNW) package for the U.S. Geological Survey's modular three-dimensional Þnite-difference ground-water ßow model, Versions MODFLOW-96 and MODFLOW-2000, 33. Open-File Report 02-293. Sacramento, California: U.S. Geological Survey.

Harbaugh, A.W., E.R. Banta, M.C. Hill, and M.G. McDonald. 2000. Modßow-2000, the U.S. Geological Survey modular ground-water model—User guide to modularization, concepts and the ground-water ßow process. Open-File Report 00-92. Reston, Virginia: U.S. Geological Survey.

Harper, J.A. 1999. Devonian. In *The Geology of Pennsylvania*, ed. C.H. Schultz, 108–127. Harrisburg: Pennsylvania Department of Conservation and Natural Resources.

Hill, M.C., and C.R. Tiedeman. 2007. *Effective Groundwater Model Calibration: With Analysis of Data, Sensitivities, Predictions, and Uncertainty.* Hoboken, New Jersey: John Wiley and Sons.

Hsieh, P.A. 2011. Application of MODFLOW for oil reservoir simulation during the Deepwater Horizon crisis. *Ground Water* 49, no. 3: 319–323. DOI: 10.1111/j.1745-6584.2011.00813.x.

Isachsen, Y.W., and W. McKendree. 1977. *Preliminary Brittle Structure Map of New York, Map and Chart Series No. 31.* Albany, New York: New York State Museum.

Jehn, P. 2011. Well and water testing—What to look for and when to look for it. In *Groundwater and Hydraulic Fracturing of the Marcellus Shale*, National Groundwater Association short course. Baltimore, Maryland.

King, G. 2010. Thirty years of gas shale fracturing: What have we learned? Paper SPE 133456 presented at the *SPE Annual Technical Conference and Exhibition*, September 19–22, 2010, Florence, Italy.

King, G.E., L. Haile, J. Shuss, and T.A. Dobkins. 2008. Increasing fracture path complexity and controlling downward fracture growth in the Barnett shale. Paper 119896 presented at the *SPE Shale Gas Production Conference*, November 16–18, 2008, Fort Worth, Texas.

Konikow, L.F. 2011. The secret to successful solute-transport modeling. *Ground Water* 49, no. 2: 144–159. DOI: 10.1111/j.1745-6584.2010.00764x.

Kramer, D. 2011. Shale-gas extraction faces growing public and regulatory challenges. *Physics Today* 64, no. 7: 23–25.

Kwon, O., A.K. Kronenberg, A.F. Gangi, B. Johnson, and B.E. Herbert. 2004a. Permeability of illite-bearing shale: 1. Anisotropy and effects of clay content and loading. *Journal of Geophysical Research* 109: B10205. DOI: 10.1029/2004/JB003052.

Kwon, O., B.E. Herbert, and A.K. Kronenberg. 2004b. Permeability of illite-bearing shale: 2. Inßuence of ßuid chemistry on ßow and functionally connected pores. *Journal of Geophysical Research* 109: B10206. DOI:10.1029/2004JB003055.

Lacombe, S., E.A. Sudickey, S.K. Frape, and A.J.A. Unger. 1995. Inßuence of leak boreholes on cross-formational groundwater ßow and contaminant transport. *Water Resources Research* 31, no. 8: 1871–1882.

Langevin, C.D., W.B. Shoemaker, and W. Guo. 2003. MODFLOW-2000, the U.S. Geological Survey modular groundwater model–Documentation of the SEAWAT-2000 version with the variable-density ßow process (VDF) and the integrated MT3DMS transport process (IMT), 43 p. Open-File Report 03-426. Tallahassee, Florida: U.S. Geological Survey.

Loyd, O.B., and L.D. Carswell. 1981. Groundwater resources of the Williamsport region, Lycoming County, Pennsylvania. Water Resources Report 51. Pennsylvania: Department of Environmental Resources.

Neuzil, C.E. 1994. How permeable are clays and shales? *Water Resources Research* 30, no. 2: 145–150.

Neuzil, C.E. 1986. Groundwater ßow in low-permeability environments. *Water Resources Research* 22, no. 8: 1163–1195.

New York State Department of Environmental Conservation (NYDEC). 2009. *Draft Supplemental Generic Environmental Impact Statement on the Oil, Gas and Solution Mining Regulatory Program—Well Permit Issuance for Horizontal Drilling and High-Volume Hydraulic Fracturing to Develop the Marcellus Shale and Other Low-Permeability Gas Reservoirs.* Albany, New York: State Department of Environmental Conservation.

Nickelsen, R.P. 1986. Cleavage duplexes in the Marcellus Shale of the Appalachian foreland. *Journal of Structural Geology* 8, no. 3/4: 361–371.

Ohio Department of Natural Resources (ODNR). 2008. Report on the Investigation of the Natural Gas Invasion of Aquifers in Bainbridge Township of Geauga County, Ohio. ODNR, Division of Mineral Resources Management.

Osborn, S.G., A. Vengosh, N.R. Warner, and R.B. Jackson. 2011. Methane contamination of drinking water accompanying gas-well drilling and hydraulic fracturing. *Proceedings of the National Academy of Sciences* 108, no. 20: 8172–8176.

Osborn, S.G., and J.C. McIntosh. 2010. Chemical and isotopic tracers of the contribution of microbial gas in Devonian organic-rich shales and reservoir sandstones, northern Appalachian Basin. *Applied Geochemistry* 25, no. 3: 456–471.

Pennsylvania Bureau of Topographic and Geologic Survey (PBTGS). 2001. *Bedrock Geology of Pennsylvania (Digital Files).* Harrisburg, Pennsylvania: PA Department of Conservation and Natural Resources.

Pennsylvania Department of Environmental Protection (PADEP). 2011. Marcellus Shale. http://www.dep.state.pa.us/dep/deputate/minres/oilgas/new_forms/marcellus/marcellus.htm (accessed June 1, 2011).

Pennsylvania Department of Environmental Protection (PADEP). 2009. Notice of Violation, Re: Gas Migration Investigation, Dimock Township, Susquehanna County, Letter from S. C. Lobins, Regional Manager, Oil and Gas Management, to Mr. Thomas Liberatore, Cabot Oil and Gas Corporation. February 27, 2009. 4 pp., PADEP, Meadville, Pennsylvania.

EPAPAV0058605

Schoell, M. 1980. The hydrogen and carbon isotopic composition of methane from natural gases of various origins. *Geochemica et Cosmochiica Act* 44, no. 5: 649–661.

Schulze-Makuch, D., D.A. Carlson, D.S. Cherkauer, and P. Malik. 1999. Scale dependence of hydraulic conductivity in heterogeneous media. *Ground Water* 37, no. 6: 904–919.

Schweitzer, R., and H.I. Bilgesu. 2009. The role of economics on well and fracture design completions of Marcellus Shale wells. Paper 125975 in SPE *Eastern Regional Meeting*, September 23–25, 2009, Charleston, West Virginia.

Shoemaker, W.B., E.L. Kuniansky, S. Birk, S. Bauer, and E.D. Swain. 2008. Documentation of a conduit ßow process (CFP) for MODFLOW-2005. U.S. Geological Survey techniques and methods, Book 6, chapter A24, 50 p. Reston, Virgina: U.S. Geological Survey.

Silliman, S., and D. Higgins. 1990. An analytical solution for steady-state ßow between aquifers through an open well. *Ground Water* 28, no. 2: 184–190.

Soeder, D.J. 2010. The Marcellus shale: Resources and reservations. *EOS* 91, no. 32: 277–278.

T.A.L. Research and Development (TAL). 1981. Geology, drill holes, and geothermal energy potential of the basal Cambrian rock units of the Appalachian Basin of New York State. In *Prepared for New York State Energy Research and Development Authority*, 54p .

West Virginia Geological and Economic Survey (WVGES). 2011. *Completed Wells—Marcellus Shale, West Virginia.* Morgantown, West Virginia: WVGES.

West Virginia Geological and Economic Survey (WVGES). 2010a. *Structural Geologic Map (Faults)—Topo of the Onondaga Limestone or Equivalent, West Virginia.* Morgantown, West Virginia: WVGES.

West Virginia Geological and Economic Survey (WVGES). 2010b. *Structural Geologic Map (Folds)—Topo of the Onondaga Limestone or Equivalent, West Virginia.* Morgantown, West Virginia: WVGES.

White, J.S., and M.V. Mathes. 2006. Dissolved-gas concentration in ground water in West Virginia, 8. Data Series 156. Reston, Virginia: U.S. Geological Survey.

Williams, J.H. 2010. Evaluation of well logs for determining the presence of freshwater, saltwater, and gas above the Marcellus shale in Chemung, Tioga, and Broome Counties, New York. ScientiÞc Investigations Report 2010–5224, 27. Reston, Virginia: U.S. Geological Survey.

Williams, J.H., L.E. Taylor, and D.J. Low. 1998. Hydrogeology and groundwater quality of the Glaciated Valleys of Bradford, Tioga, and Potter Counties, Pennsylvania. Water Resource Report 68. Pennsylvania Dept of Conservation and Natural Resources and U.S. Geological Survey.

Wunsch, D. 2011. Hydrogeology and hydrogeochemistry of aquifers overlying the Marcellus shale. In *Groundwater and Hydraulic Fracturing of the Marcellus Shale*, National Groundwater Association short course. Baltimore, Maryland.

EPAPAV0058606